ENERGY LOSS OF HIGH ENERGY ELECTRONS IN ALUMINUM

ROYCE DUANE MILLER

ENERGY LOSS OF HIGH ENERGY ELECTRONS

IN ALUMINUM

by

Royce Duane Miller
Major, United States Army
B.S., South Dakota School of Mines and Technology, 1956

Submitted in partial fulfillment of the
requirements for the degree of

MASTER OF SCIENCE IN PHYSICS

from the

NAVAL POSTGRADUATE SCHOOL
June 1968

ABSTRACT

High energy electrons from the USNPGS LINAC were used to study the energy distribution characteristics of the electrons before and after passage through various thicknesses of aluminum absorbers. Data was taken for initial energies between 50 and 100 MeV, and for absorbers of thicknesses between 0.28 gm/cm^2 and 3.1 gm/cm^2. The results were compared with the theory of Blunck and Westphal, and the experimental measurements of Breuer. Geometrical factors involved in the experimental arrangement were found to have had a pronounced effect on the measurements, and refinements to the experimental conditions for future measurements of this type are indicated. Preliminary work in this direction shows that the half widths and most probable energy losses given by the theory are confirmed within experimental errors.

TABLE OF CONTENTS

LIST OF TABLES

LIST OF ILLUSTRATIONS

I. INTRODUCTION

High energy electrons are known to lose energy in passing through material media. These losses occur mainly through ionization and excitation when the passing electrons interact with the atomic electrons and through radiation (bremstrahlung). While interactions also occur with atomic nuclei, the losses due to such interactions are normally negligible due to the limited energy transfer resulting from the differences in mass between the electrons and the nuclei. The principal effect of interactions with nuclei is to lengthen the path of electrons in passing through a layer of material due to multiple scattering thus increasing the losses due to radiation, ionization, and excitation.

Several authors have treated this problem theoretically (1, 2, 3, 4, 5, and 9), and a limited number of measurements are in the literature (6, 7, 8, and 12); however, no reported measurements on aluminum have been carried out in the energy range of 60 - 100 MeV.

The Naval Postgraduate School electron linear accelerator (LINAC) provides the capability to make such measurements. A series of measurements has therefore been carried out in this energy range to determine the most probable energy loss and the energy loss distribution characteristics. According to the theoretical considerations which will be discussed in section II, the energy loss of electrons in passing through relatively thin absorbing layers can be characterized by the most probable energy loss Q_p and the half width

HW of the distribution. The half width is defined as the energy width of the distribution at one half the maximum intensity.

II. THEORETICAL CONSIDERATIONS

Blunck and Westphal (B&W) (1) have developed a theoretical distribution for the energy loss due to ionization, excitation, and radiation which is based on the works of Landau (2), Blunck and Leisegang (3), Eyges (4), and Bethe and Heitler (5). Their distribution is given as a function of the dimensionless parameter λ which is a linear function of the energy loss Q. The parameter λ is defined by:

$$\lambda = \frac{Q - \overline{Q}}{aR} + \ln \frac{E_i}{aR} - 1.116$$

Here $\overline{Q}$ is the average energy loss through ionization in MeV suffered by the electrons of initial energy E_i(MeV) in passing through an absorber of thickness R(cm). The constant a is a function of the atomic number Z, the atomic weight A and the density ρ (gm/cm^2) of the absorbing medium, and of the velocity β = v/c of the passing electron. The expression for a is given by B&W as:

$$a = 0.154 \frac{Z}{A} \cdot \frac{\rho}{\beta^2} \left(\frac{\text{MeV}}{\text{cm}}\right)$$

For the probability distribution W(Q)dQ B&W give:

$$W(Q)dQ = B \times \left(\frac{aR}{E_i}\right)^{\alpha R} \times F_{\alpha R,\, b^2}(\lambda)\, d\lambda$$

with:

$$F_{\alpha R,\, b^2}(\lambda) = \Gamma(\alpha R+1)\left(\tfrac{1}{2}\right)^{\frac{\alpha R}{2}} \cdot \sum_n \frac{C_n \gamma_n e^{-\frac{(\lambda-\lambda_n)}{2(b^2+\gamma_n^2)}}}{\sqrt{(b^2+\gamma_n)^{1-\alpha R}}} D_{-\alpha r}\left(\frac{\sqrt{2}(\lambda-\lambda_n)}{\sqrt{b^2+\gamma_n^2}}\right)$$

Here the term B is a normalizing constant. The terms C_n, γ_n, λ_n, are constants given for the appropriate values of the summation integer n as indicated in Table I. α is a constant which determines the radiation contribution to the distribution and was taken by B&W from the works of Bethe and Heitler (5). The value of the constant α is determined for the absorbing material by:

$$\alpha = 1.40 \times 10^{-3} \times \frac{Z}{A}^2 \times \rho \left[4/3 \ln (183/Z^{1/3}) + 1/9 \right] \left(\frac{1}{cm} \right)$$

TABLE I. Distribution Constants

n	1	2	3	4
C_n	0.174	0.058	0.019	0.007
γ_n	0.0	3.0	6.5	11.0
λ_n	1.8	2.0	3.0	5.0

The term b^2 is obtained from Blunck and Leisegang (3) and can be written in the form:

$$b^2 = \frac{3.0}{aR} \cdot \sum_m \frac{I_m N_m}{Z} \cdot \ln \left(\frac{2E_i}{I_m (1 - \beta^2)} \right)$$

in which the summation is over the m different ionization potentials of the atomic electrons of the absorber. N_m is the number of electrons per atom or molecule of the absorber with the ionization potential I_m. $D_{-\alpha R}\left(\frac{\sqrt{2}(\lambda - \lambda_n)}{-\sqrt{b^2 + \gamma_n^2}}\right)$ is the parabolic cylinder function of the indicated arguments. B&W have calculated the function $F_{\alpha R, b^2}(\lambda)$ for b^2 values of 0, 3, 6, and 9, and αR values of 0, 0.05, 0.10, 0.15,

0.20, and 0.25 as a function of λ for values of λ of approximately -7 to +15; and they have presented the results of these calculations graphically. It is to be noted that for a given initial energy and absorber thickness, the distribution $F_{\alpha R, b^2}(\lambda)$ is directly proportional to W(Q) with all other terms being involved only in the normalization. Since λ is linearly proportional to Q one can write:

$$Q = (aR)\lambda + Q_o$$

or

$$\lambda = \frac{Q - Q_o}{aR}$$

where

$$Q_o = \overline{Q} - aR \times \ln\left(\frac{E_i}{aR}\right) + 1.116\,(aR)$$

is the energy loss corresponding to λ equals zero.

In evaluating $\overline{Q}$ the average energy loss due to ionization and excitation, the equations given by Sternheimer (9) are used. These equations take into account the density effect due to polarization of the medium. Sternheimer's equations for the average energy loss can be combined and written in the form:

$$\overline{Q} = \frac{A_s t}{\beta^2}\left[B_s + 0.43 + \ln E_i - \beta^2 - C - a_s\left(X_1 - \log_{10}\frac{p}{mc}\right)^{m_s}\right]$$

In these last two equations the terms A_s, B_s, C, X_1, a_s, and m_s are constants which depend upon the absorbing material. Sternheimer (9, c) gives these constants for aluminum as $A_s = 0.074$, $B_s = 16.77$, $C = -4.21$, $m_s = 3.51$, $a_s = 0.0906$, and $X_1 = 3.0$. By the relativistic mass energy relationship the quanity p/mc can be expressed as:

$$\frac{p}{mc} = \frac{pc}{mc^2} = \frac{\sqrt{E^2 + 2mc^2 E}}{mc^2}$$

which shows the energy dependence of this term.

Sternheimer (9, b) also gives an equation for the most probable energy loss Q_{pi} due to ionization and excitation losses which is of interest in comparing with the most probable loss determined from the theory of B&W and the experiment for a comparison of the relative effects of ionization and excitation, and radiation on the most probable energy loss. This equation from Sternheimer can be written in the form:

$$Q_{pi} = \frac{A_s t}{\beta^2}\left[B_s + 1.06 + \ln\left(\frac{A_s t}{\beta^2}\right) - \beta^2 - C - a_s\left(X_1 - \log_{10}\frac{p}{mc}\right)^{m_s}\right]$$

This equation can for a given E_i under the assumption of small energy losses be written in the form:

$$Q_{pi} = K_1 t + K_2 t \ln t$$

where K_1 and K_2 are constants which can be determined from the previous equation. This latter equation shows that contrary to the interpretation of Breuer (12), the most probable loss due to ionization and excitation Q_{pi} does not vary linearly with the thickness of the absorber. Figures 1 and 2 show this variation from linear behavior by showing respectively Q_{pi}/t as a function of E_i for selected thicknesses and Q_{pi} as a function of t at a constant energy of E_i equals 70.00 MeV. Actually as can be seen from figure 1, figure 2 represents the theoretical dependence of Q_{pi} on thickness with good accuracy for a wide range of energy (from 50 to 100 MeV the theoretical deviations from this curve do not exceed ±.5%).

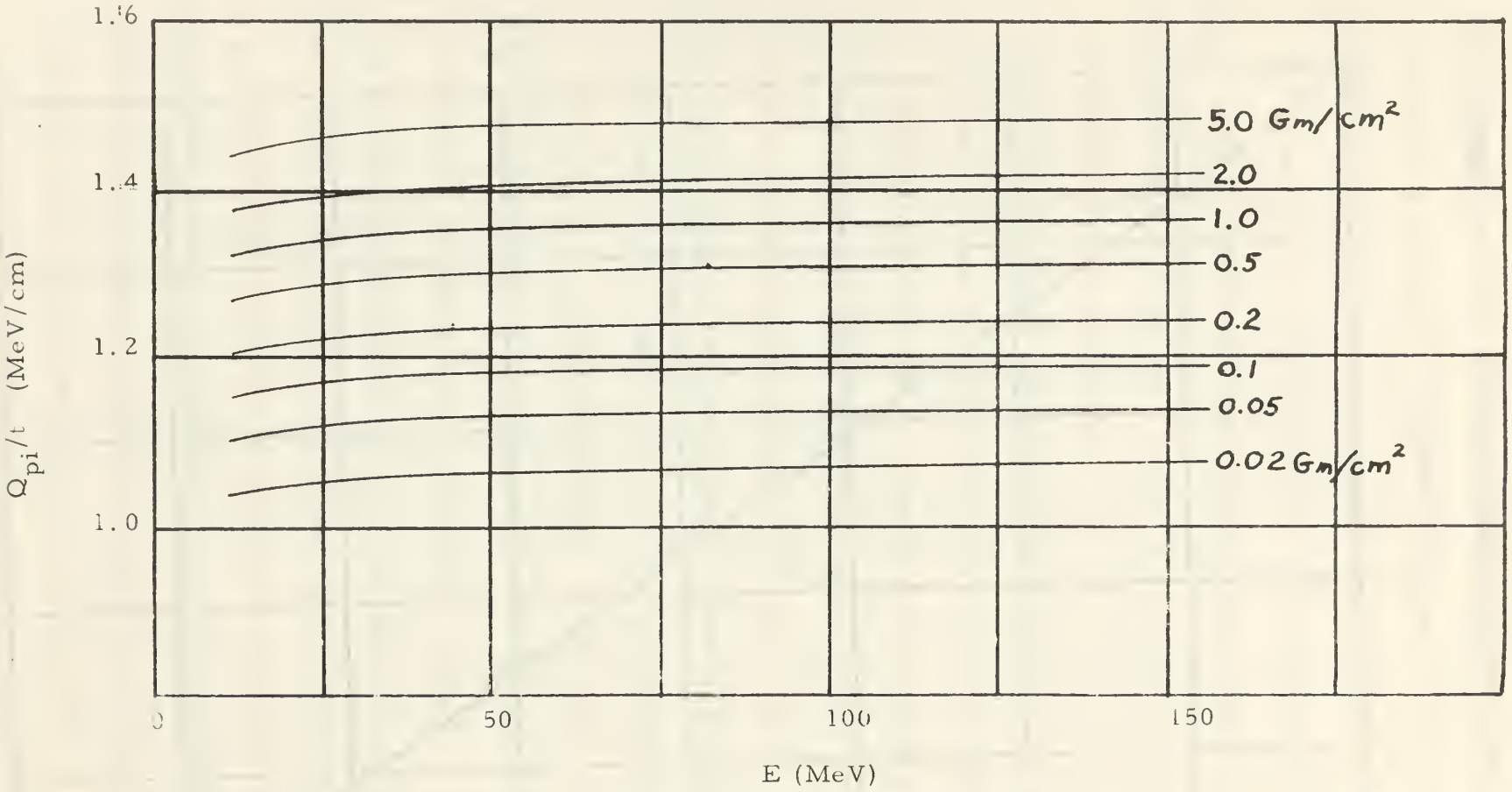

FIGURE 1 Most Probable Ionization Loss Rate

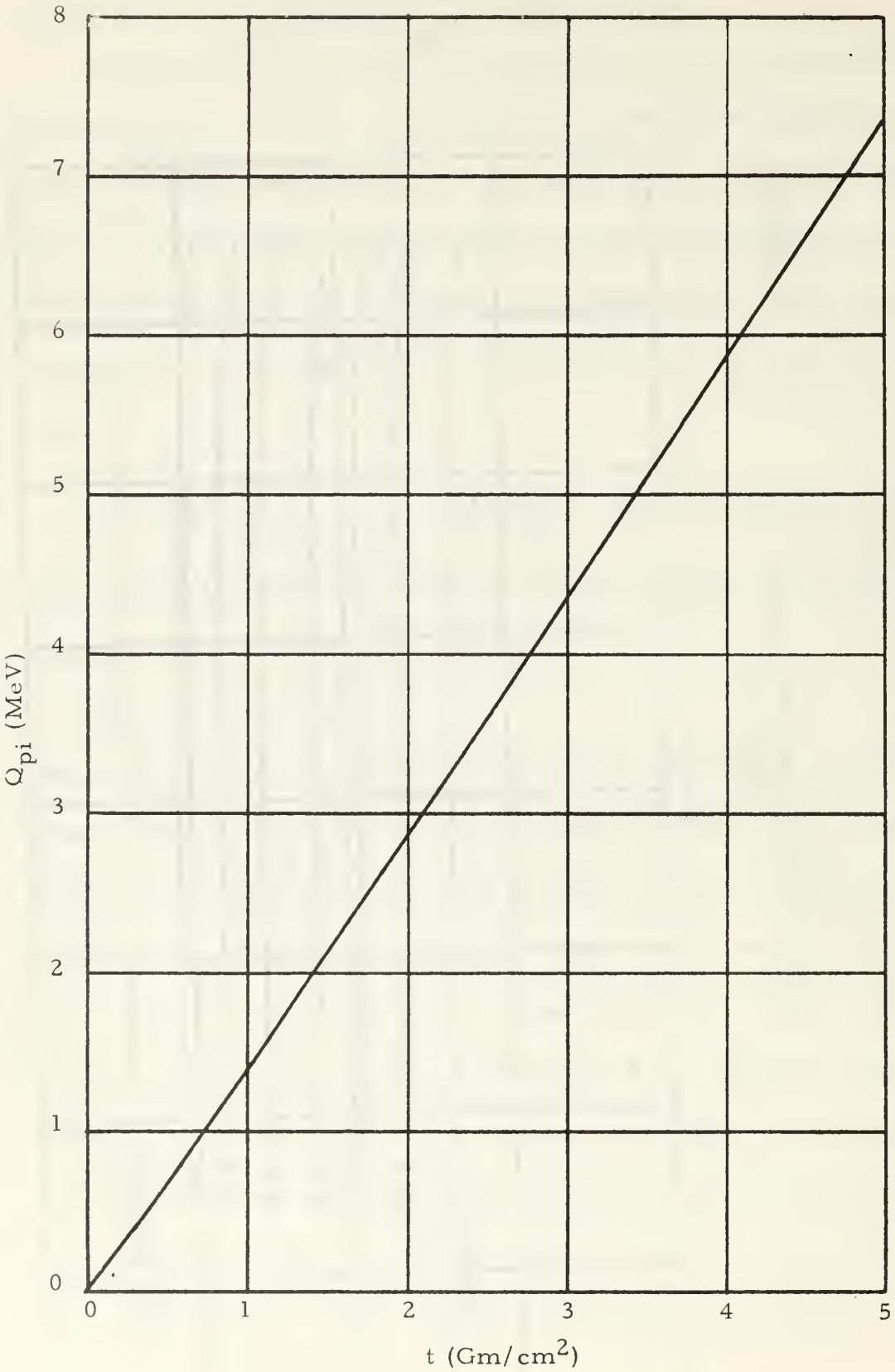

FIGURE 2 Most Probable Ionization Loss

The characteristics of the distribution given by B&W can to a limited extent be specified by giving the half width and the energy of the maximum. Figure 3 is derived from the work of B&W and shows the variation of the half width with respect to the related parameters. The diagonal straight line in figure 3 gives the relation between aR and $\varkappa$ R for Al by use of the left and top scales so that only aR and b^2 need be calculated. The curved lines give the half widths of the distributions for selected values of b^2 as a function of $\varkappa$ R by use of the left and bottom scales. To estimate the monoenergetic half width one first calculates the values of aR and b^2; then by finding the point on the straight line which corresponds to the calculated aR value $\varkappa$ R is determined. With this value of $\varkappa$ R one finds the appropriate value of b^2 by interpolation and reads the value of HW/aR from the bottom scale. Multiplying this value by the computed aR gives the half width in MeV. From figure 4 the most probable energy loss according to B&W can also be obtained and thus the location of the maximum is determined. These two characteristics give, however, only partial information of the distribution as can be implied from figure 3; in figure 3 one sees that the same half width could be expected over a range of values for aR, $\varkappa$ R, and b^2. The points of intersection of the curves in figure 3 with the $\varkappa$R = 0 line represent the solutions of Blunck and Leisegang for the case of radiation being ignored and at $b^2 = 0$ also the solution of Landau.

The effects of multiple scattering of the electrons within an absorbing layer have been treated by Yang (10). He gives a theoretical

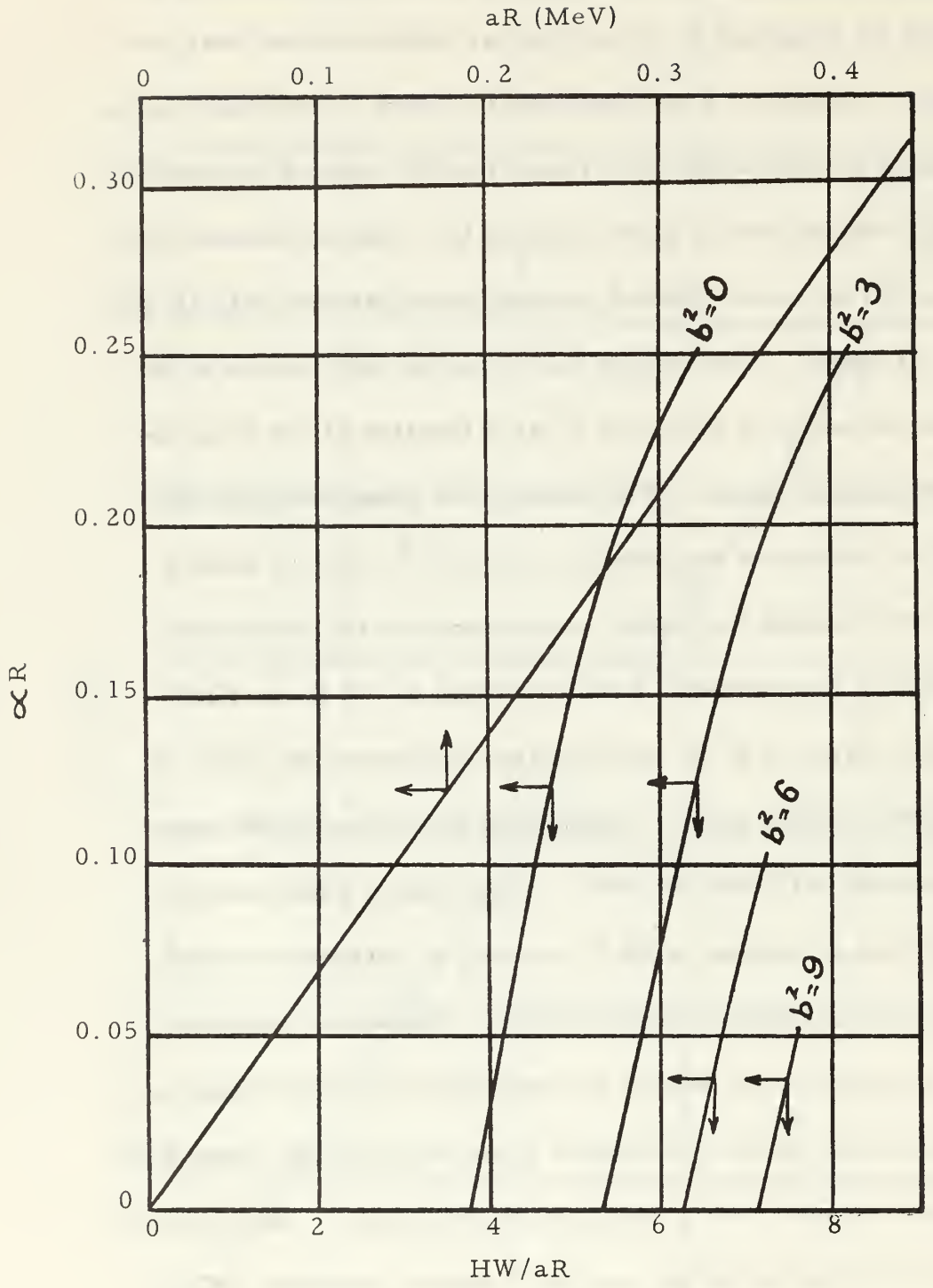

FIGURE 3 Blunck and Westphal Half Width

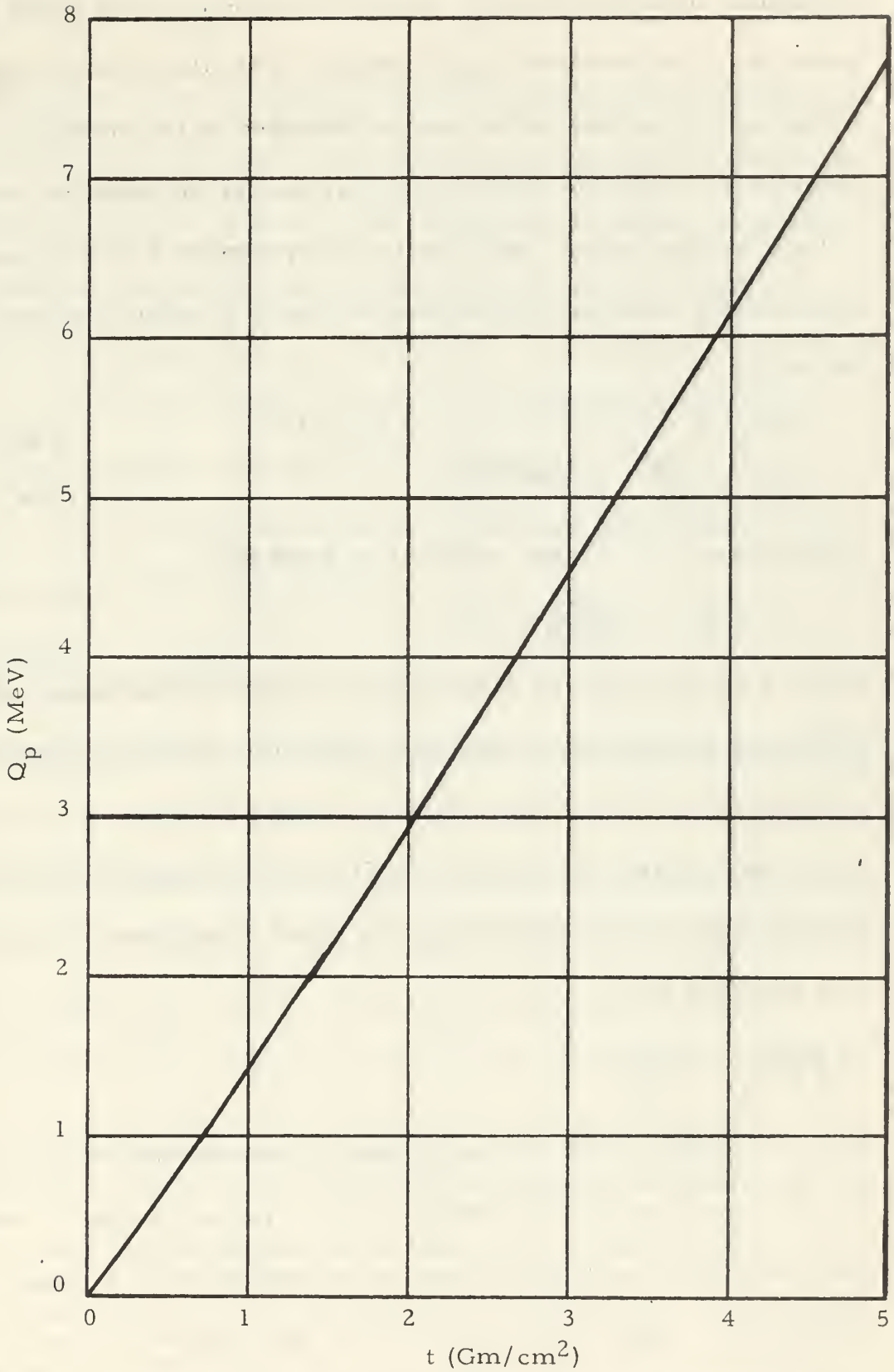

FIGURE 4 Most Probable Ionization and Radiation Loss

probability distribution for the path lengthening in terms of the parameter V. In an asymtotic approximation to his theory he gives the following expressions for the ranges indicated as the probability distribution for V for the case of electrons leaving the absorber parrallel to their incident paths. He indicates an agreement between these approximate relations and the detailed theory to within less than 1% deviation.

$$B(V) = 4\,\pi^{-\frac{1}{2}}\,V^{-5/2}\,(1 - V/2)\,e^{-1/V} \qquad (V \leqslant 1.0)$$

$$B(V) = \frac{\pi^2}{2}\,e^{-\pi^2 V/4} \qquad (V \geqslant 1.0)$$

The parameter V in these relations is given by:

$$V = 2(\triangle T)\left(\frac{2PCB}{21MeV}\right) / T^2$$

where T is the thickness of the layer in radiation lengths and ($\triangle T$) is the path lengthening in radiation lengths (the radiation length for aluminum is given in Rossi (11) as 24.4 gm/cm^2).

From a graphic portrayal of B(V) given by Yang, the most probable relative path lengthening can be shown to be given with acceptable accuracy by:

$$\left(\frac{\triangle t}{t}\right)_p = \frac{0.93t}{E_i^{\,2}}$$

since at energies of 50 MeV and higher the approximation pc equals E and β equals unity is acceptable for this type calculation. Yang also gives in the work cited above an expression to the average to the average path lengthening for the parallel path case which can be used to show that the average relative path lengthening is given to good accuracy by:

$$\left(\frac{\Delta t}{t}\right)_{av} = \frac{1.53t}{E_i^2}$$

By integration of the second expression for B(V) given above from an arbitrary V greater than 1.0 to infinity, one can estimate the probability of an electron suffering path lengthening of greater magnitude than that corresponding to the arbitrarily chosen V. If such integration is performed and the probability is restricted to 10% (or 0.10) one can solve the resulting equation in V for the path lengthening which corresponds to the maximum lengthening for 90% of the electrons. This type calculation yields for the maximum relative path lengthening of 90% of the electrons:

$$\left(\frac{\Delta t}{t}\right)_{90} = \frac{3.0t}{E_i^2}$$

which means that 90% of the electrons will suffer lesser path lengthening than that indicated by the last equation.

The theoretical significance of the last three equations for multiple scatter path lengthening is that the effect should be negligible for the current measurements. Since the thicknesses are less than 5 gm/cm^2 and the energies are all above 50 MeV for the range of the current measurements, the predicted percentage increases in path length are for the most probable path lengthening less than 0.2%, for the average path lengthening less than 0.3%, and for the maximum path lengthening of 90% of the electrons less than 0.6%. From these equations for path lengthening it can then be seen that the effects of multiple scattering are in general small except for the case of low

energy or large layer thickness, and these are conditions that in general would violate the assumption of small energy loss in comparison to the initial energy.

III. EXPERIMENTAL PROCEDURE

The experimental measurement of the energy loss requires a source of high energy electrons which is provided by the LINAC, and a means of determining the energy distribution of these electrons both before and after passage through the selected absorbers. The energy distribution was measured with the 16 inch magnetic spectrometer and the counting system used for electron scattering experiments; this system is described by Kenaston, Luke, and Sones (13).

Due to the limitations of counting rate imposed by the counting system, the spectrometer could not be used at a zero degree position to directly measure the electron energy distribution because the beam intensity could not be reduced sufficiently to permit this type of operation. Consequently a scattering foil was placed in the electron beam to provide an acceptable electron flux into the spectrometer at an off beam line position as was done by Breuer (12)(See figure 5). The absorbers were then placed between the scattering foil and the spectrometer when measuring the energy distribution of the electrons passing through the absorber.

In order that the absorbers could be readily changed inside the evacuated scattering chamber, a remotely controlled rotating wheel type of mounting was installed and used in most of the measurements. This wheel permitted the mounting of up to 8 different absorbers at one time with an additional blank space provided for taking the distribution of the initial electron energy. Due to the limitations imposed

by the size of the scattering chamber, the absorbers mounted on this wheel were located approximately 22 cm from the scattering foil.

One measurement was carried out with the absorber mounted on the target ladder which held the scattering foil in such a way that the absorber was only approximately 3 cm from the scatterer but out of the main beam line. The use of the mounting wheel with the absorbers at the 22 cm position can be seen to have been illadvised by comparing the results in figures 8 and 9.

Prior to the start of these measurements, the spectrometer had not been connected directly to the scattering chamber. Instead the chamber had a series of windows of thin mylar as did the entrance to the spectrometer; between the spectrometer and the scattering chamber this previous arrangement had also left an air space of approximately 5 inches. Since it was expected that these intervening materials would cause significant energy loss and broadening of the distributions, an adapter was designed and fabricated which permitted the removal of the windows between the scattering chamber and the spectrometer to provide a free path in vacuum for the electrons from the scattering foil and absorbers into the spectrometer. Measurements of the distributions with and without this coupling proved that significant broadening did occur when the windows and air space were in the path; this effect proved to be about 30% broadening of the initial energy distribution with a corresponding reduction in the maximum intensity. All measurements were therefore carried out with the vacuum coupling.

The spectrometer and counting system have only a capability to measure the intensity of a small energy interval at one time; therefore, it was necessary to take several readings at different intervals to construct the energy distributions. In order that the individual measurements which make up any one distribution could be properly weighted, a secondary emission monitor (SEM) was used to integrate the total electron beam flux so that each count was based on the same total charge passing through the scattering foil. The SEM therefore provided the necessary standard for relating the individual measurements.

A typical plan view of the experiment is shown in figure 5. The scattering foils were made of 3.3 mil aluminum foil. The absorbers were machined from electrical conductor grade aluminum of greater than 99.4% purity.

Table II gives the experimental parameters used for the energy loss measurements. The measurements at approximately 53.8 MeV were taken to permit comparison with the results of Breuer (12).

TABLE II. Experimental Parameters

E_i (MeV)	t (gm/cm^2)	absorber position
53.7, 70.1, 89.4	0.282	22 cm
53.7, 70.1, 89.4	0.711	22 cm
53.7, 70.1, 89.4	1.041	22 cm
53.9, 70.1, 89.4	1.522	22 cm
53.9, 70.1, 89.4	2.072	22 cm
53.9, 70.1, 89.4	3.038	22 cm
53.8	1.522	3 & 22cm

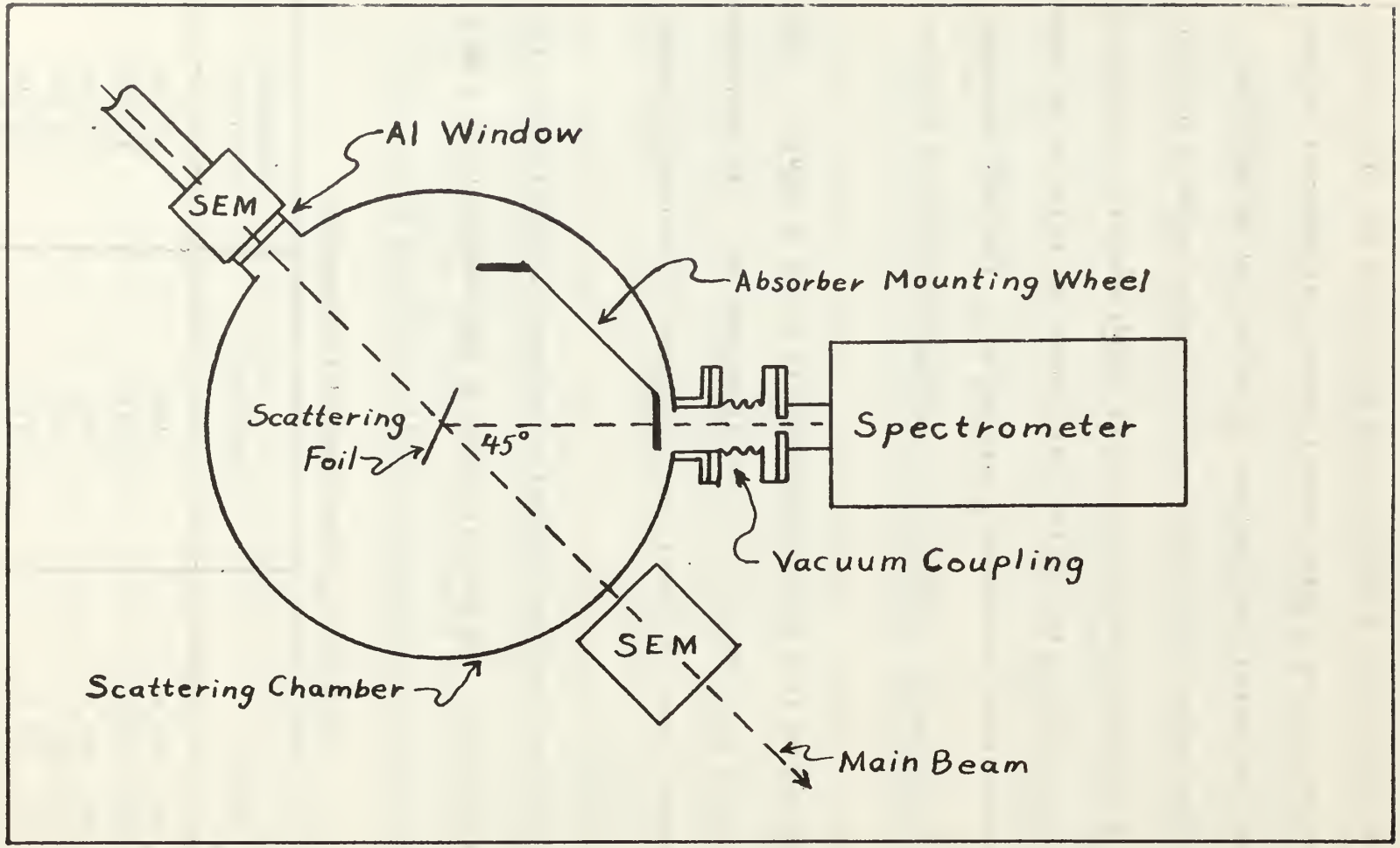

FIGURE 5 Plan View of Experimental Arrangement

The data taken for the energy distributions were the spectrometer energy setting, the counts recorded for a standard beam integration of 1 microcoulomb by charging a 10 microfarad capacitor connected to the SEM (effi ciency approx. 10%) to 10 millivolts, and the elapsed time in seconds for the integration. This data permitted appropriate corrections to be made when required due to high counting rate. Background counts were also taken without the scattering foil in place to evaluate the effects of endstation background on the experimental counts. These backgrounds proved to be negligible within the energy ranges of interest.

Further measurements were attempted with the absorbers mounted close to the scattering foil, but technical problems developed in the accelerator which precluded the accomplishment of such measurements in time for inclusion in this paper.

IV. TREATMENT OF DATA

Since the theory presented in section II is based on initially monoenergetic electrons, and the data (See figure 6) indicate that the initial energy distribution, while essentially monoenergetic with respect to total energy (half width approx. 0.57% of total energy), cannot be considered as monoenergetic with respect to the relatively small energy losses. To determine the theoretical distribution resulting from the passage of the electrons with the initial energy distribution measured requires a folding of the measured distribution with the theoretical monoenergetic distribution. If the mathematical form of the initial distribution, way F(E), were known, the theoretical resulting distribution would be given by:

$$G(E_f) = \int_{E_i} W(E_i - E_f) \times F(E_i)\, dE_i$$

where the integration is over the range of the initial energy distribution. However, the exact mathematical form of the initial distribution is not known, and even if it were known, in all probability the integration could not be readily evaluated. Rather than to attempt to fit the initial distribution to a mathematical function, the resulting theoretical distributions are, therefore, approximated by representing the continuous distributions by histograms with each element of the histogram small compared to the width of the theoretical monoenergetic distribution and with the energy increments of both distributions of equal width.

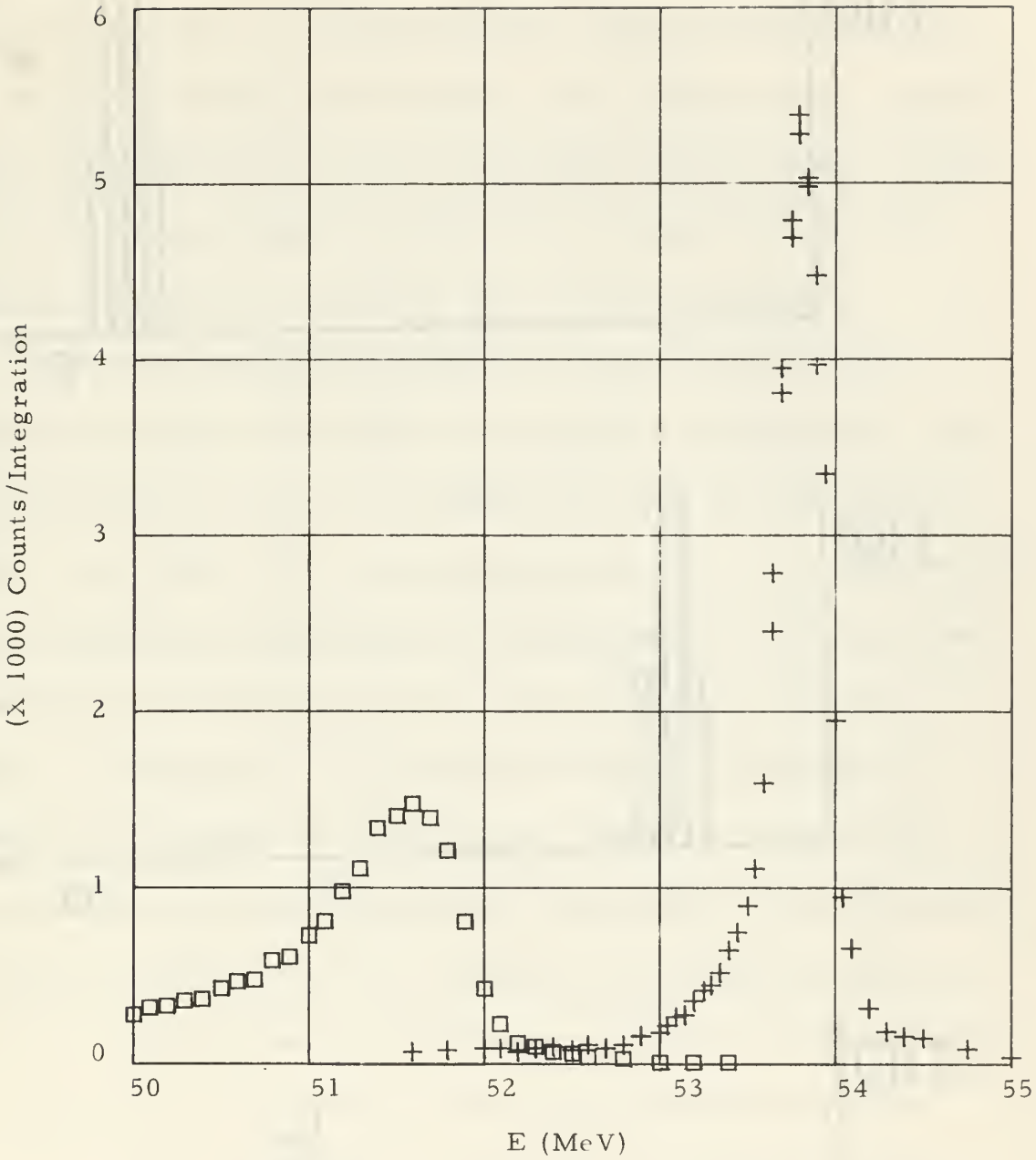

FIGURE 6 Initial and Final Energy Distributions

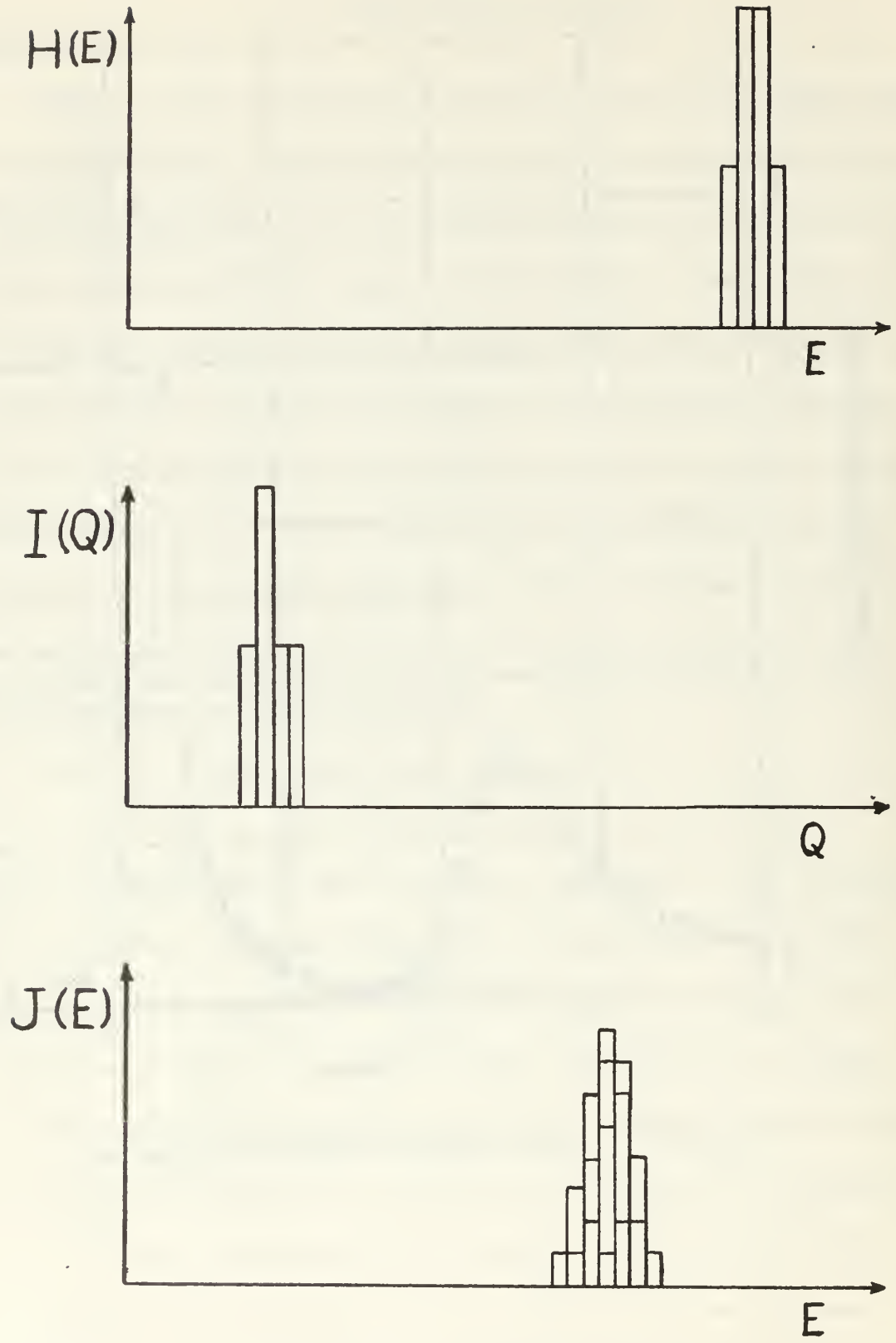

FIGURE 7 Histogram Distribution Illustration

Figure 7 shows two simple histograms, H(E) and I(Q), being operated to produce a resulting histogram, J(E). If I(Q) represents the theoretical energy loss distribution of a "monoenergetic" group of electrons and H(E) the frequency distribution of the incident electrons in various "monoenergetic" levels of small energy width, then the resulting distribution is given by J(E) if properly normalized.

The above technique was applied to the data by selecting the appropriate curves from B&W for the thickness of the absorber and calculating the theoretical distributions by use of the IBM 360 computer at the NPGS. The resulting theoretical curves were normalized to the experimental peak amplitude and compared with the measured distributions (See figures 8 and 9). The graphical presentations of B&W are truncated at $\lambda = 15$ which in all cases of interest fits within the half width, but this truncation results in low theoretical distributions below the half maximum point on the low end of the final energy distribution curve. In an attempt to overcome this discrepancy to a limited extent, the distribution curves were extrapolated by an exponential extension fitted to the slope of the B&W curves at $\lambda = 15$. This extrapolation is expected to give better agreement with measured data for the larger energy loss regions without significant effect on the predicted half widths.

Table III gives the values of the distribution parameters to be used for the B&W theory for the absorbers and energies used. It can be seen from this table that for most of the absorbers and energies

TABLE III. Distribution Parameters

t (gm/cm^2)	E_i (MeV)	b^2	aR (MeV)	R
0.282	53.7	0.893	0.0209	0.0146
	70.1	0.927	0.0209	0.0146
	89.4	0.959	0.0209	0.0146
0.711	53.7	0.354	0.0528	0.0369
	70.1	0.368	0.0528	0.0369
	89.4	0.380	0.0528	0.0369
1.041	53.7	0.242	0.0772	0.0540
	70.1	0.251	0.0772	0.0540
	89.4	0.250	0.0772	0.0540
1.522	53.8/53.9	0.165	0.1130	0.0790
	70.1	0.171	0.1130	0.0790
	89.4	0.178	0.1130	0.0790
2.072	53.9	0.122	0.1538	0.1076
	70.1	0.126	0.1538	0.1076
	89.4	0.130	0.1538	0.1076
3.038	53.9	0.083	0.2255	0.1577
	70.1	0.086	0.2255	0.1577

the parameter b^2 is considerably smaller than 3 and the approximation of b^2 equals zero would not be expected to give significant errors. The effect of b^2 is shown in figure 8 by plotting the theoretical final distributions resulting from the initial distribution measured at 53.8 MeV as calculated for b^2 values of zero and 3 for a 1.522 gm/cm^2 absorber. The actual theoretical value of b^2 for the case shown is 0.165.

V. RESULTS

The theoretically predicted and the experimentally measured values of the most probable energy loss and half widths for the various thicknesses of absorbers and initial energies are tabulated in table IV. The column headed S under Qp gives the values obtained from the Sternheimer equation.

Only in the case of the 1.522 gm/cm^2 absorber at 53.8 MeV which is marked by an asterix is there any reasonable agreement in the results on half width; this one distribution was measured with the absorber at approximately 3 cm from the scattering foil and thus much nearer the focal point of the spectrometer. All other distributions were measured with the absorbers at a position approximately 22 cm from the scattering foil and focal point. This effect will be discussed in section VI.

The most probable energy loss results are systematically higher than those of either B&W of Sternheimer but seem to follow the theory of B&W more closely. It is believed that experimental geometry played a role in this discrepancy as well as in the half widths. Section VI contains further discussion on this point.

The experimental distribution for the 53.8 MeV distribution for the 1.522 gm/cm^2 absorber is shown in figure 6 with the initial energy distribution. The most probable energy loss is measured as the energy difference in the locations of the maxima of the two distributions.

TABLE IV. Energy Loss Distribution Characteristics

		Q_p (Mev)			HW (MeV)	
$t(gm/cm^2)$	E_i(MeV)	B&W	S	Experiment	Theory	Experiment
0.282	53.7	0.367	0.356	$0.40^{+}_{-}.04$	0.42	$0.60^{+}_{-}.04$
	70.1	0.368	0.357	$0.44^{+}_{-}.05$	0.46	$0.63^{+}_{-}.04$
	89.4	0.368	0.357	$0.39^{+}_{-}.06$	0.42	$0.70^{+}_{-}.08$
0.711	53.7	0.971	0.947	$1.05^{+}_{-}.07$	0.52	$0.93^{+}_{-}.07$
	70.1	0.973	0.949	$1.09^{+}_{-}.09$	0.60	$1.10^{+}_{-}.06$
	89.4	0.974	0.950	$1.06^{+}_{-}.08$	0.67	$1.15^{+}_{-}.10$
1.041	53.7	1.453	1.416	$1.58^{+}_{-}.07$	0.66	$1.10^{+}_{-}.07$
	70.1	1.455	1.419	$1.64^{+}_{-}.10$	0.75	$1.49^{+}_{-}.10$
	89.4	1.456	1.420	$1.61^{+}_{-}.09$	0.82	$1.54^{+}_{-}.10$
1.522	53.8*	2.174	2.115	$2.21^{+}_{-}.04$	0.81	$0.92^{+}_{-}.05$
	53.8	2.174	2.115	$2.29^{+}_{-}.12$	0.81	$1.50^{+}_{-}.12$
	53.9	2.174	2.115	$2.39^{+}_{-}.10$	0.88	$1.42^{+}_{-}.15$
	70.1	2.177	2.118	$2.34^{+}_{-}.10$	0.98	$1.55^{+}_{-}.15$
	89.4	2.179	2.120	$2.35^{+}_{-}.14$	1.14	$1.60^{+}_{-}.10$
2.072	53.9	3.010	2.926	$3.30^{+}_{-}.15$	1.09	$1.92^{+}_{-}.10$
	70.1	3.014	2.931	$3.25^{+}_{-}.14$	1.20	$1.80^{+}_{-}.20$
	89.4	3.017	2.934	$3.37^{+}_{-}.15$	1.44	$1.95^{+}_{-}.15$
3.038	53.9	4.530	4.376	$4.80^{+}_{-}.20$	1.65	$2.00^{+}_{-}.20$

Figure 8 shows this same experimental distribution for the 1.522 gm/cm^2 absorber along with the theoretical distributions calculated by the B&W theory for b^2 values of zero and 3. The calculated b^2 for this energy and absorber is 0.165. The comparable distribution for this absorber positioned 22 cm from the scattering foil is shown in figure 9. Comparison of these two figures shows the detrimental effect of the absorber being located significant distances from the spectrometer focal point.

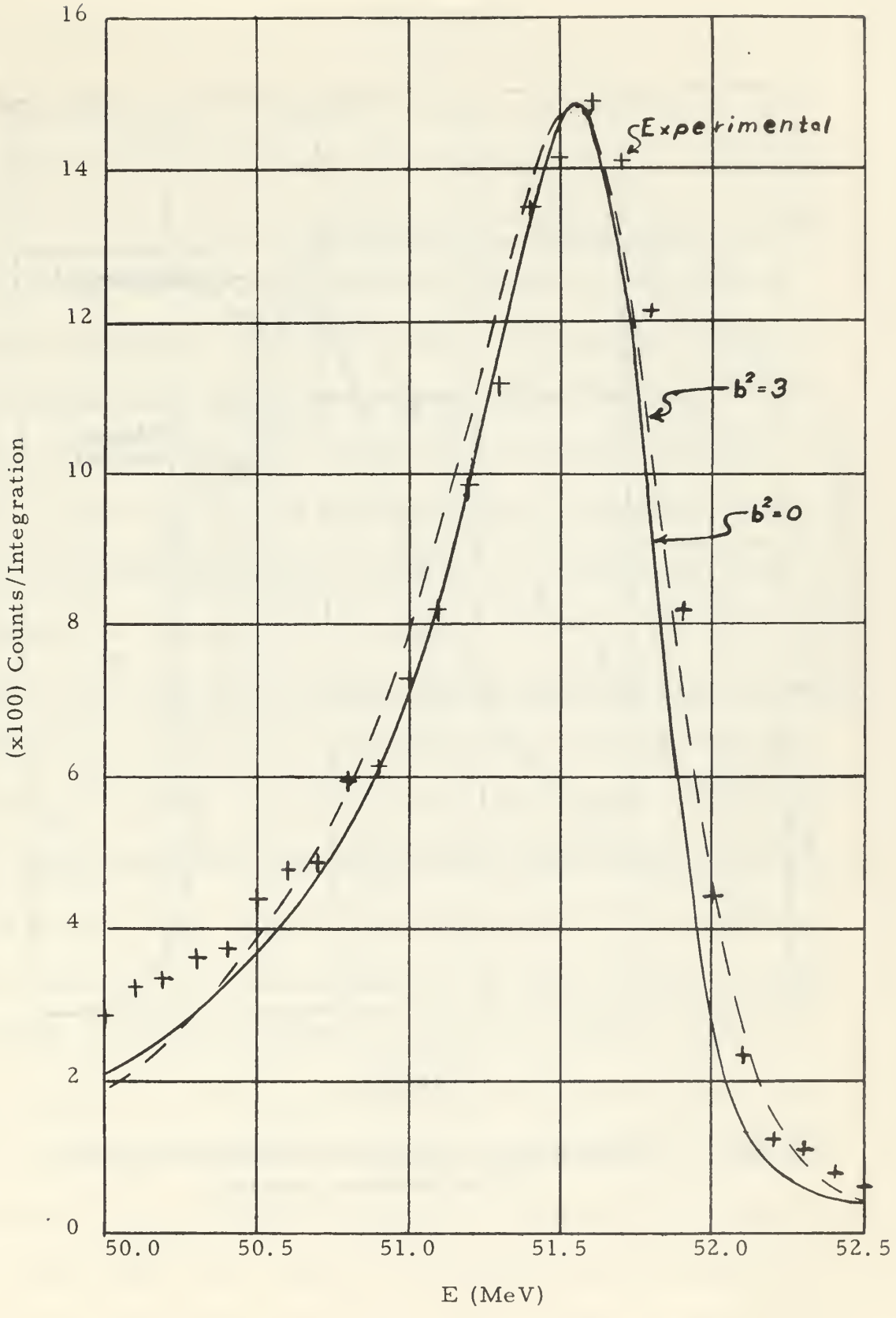

FIGURE 8 Theoretical and Experimental Final Distribution
(3 cm absorber position)

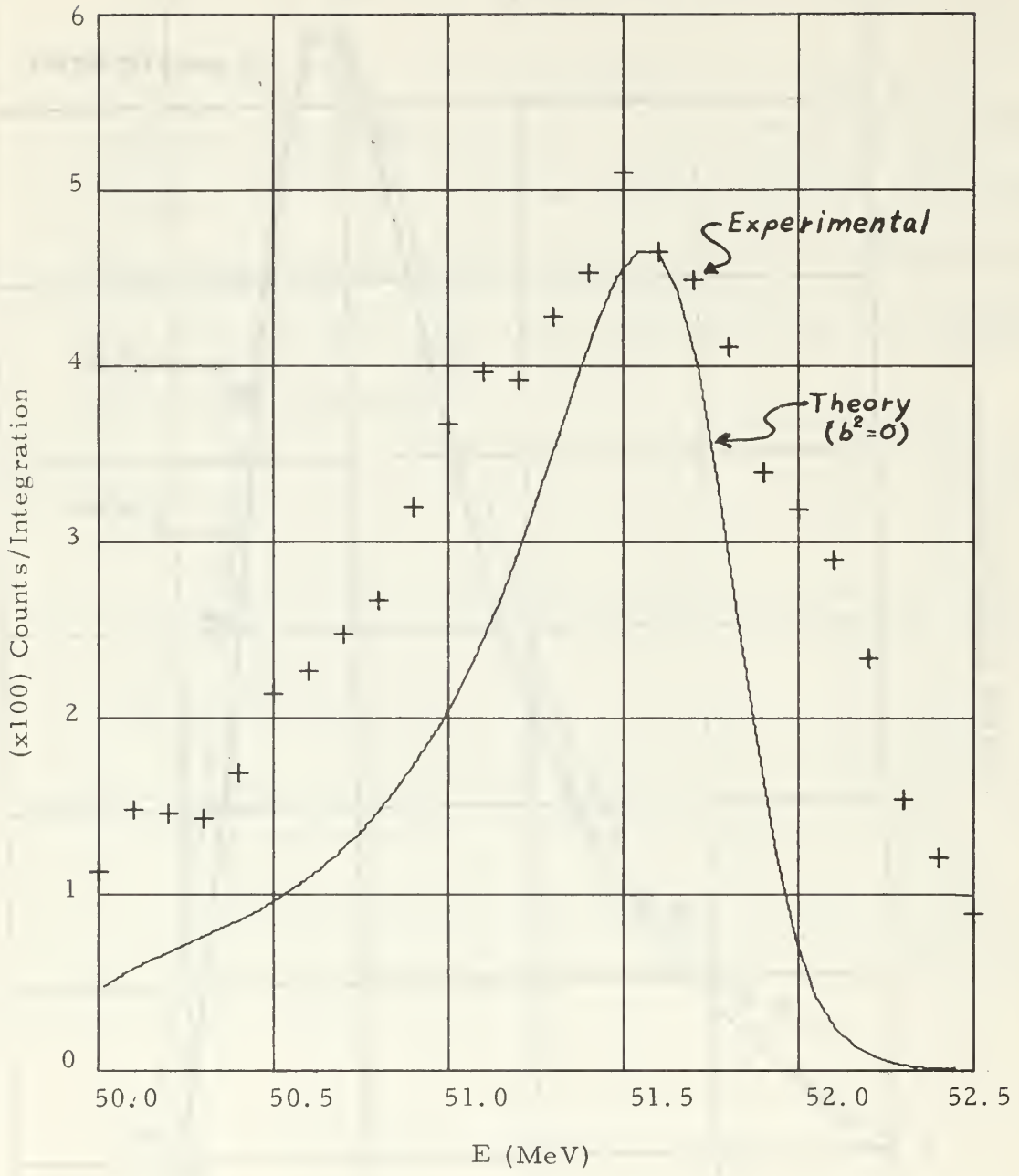

FIGURE 9 Theoretical and Experimental Final Distribution (22 cm absorber position)

VI. DISCUSSION

The general lack of agreement between the experimental measurements and the theoretically predicted half widths is explainable in terms of spectrometer resolution errors induced by the absorbers scattering electrons in single scattering events in such a manner that the spectrometer sees these scattered electrons as coming from virtual source points far removed from the focal point. Figure 10 illustrates this effect by showing how electrons assumed to have the same energy would pass through the spectrometer. The paths that show scattering are projected back to the vertical plane containing the focal point of the spectrometer to their virtual source points. From this one can see that for an electron on any given path incident on the absorber so as to make such a scattering, that the further the absorber is located from the plane containing the focal point of the spectrometer the further the virtual source point will be from the focal point. Since the focusing properties of the spectrometer are such that it focuses points at the source to points at the detector, displacement of the apparent source points through scattering will result in even monoenergetic electrons appearing to have an energy distribution. This then shows qualitatively how the geometry of the experiment caused the discrepancy in half widths.

With regard to the tendency of the measured most probable energy losses to exceed the theoretical systematically, one must consider that the broadening of the distributions first of all makes the

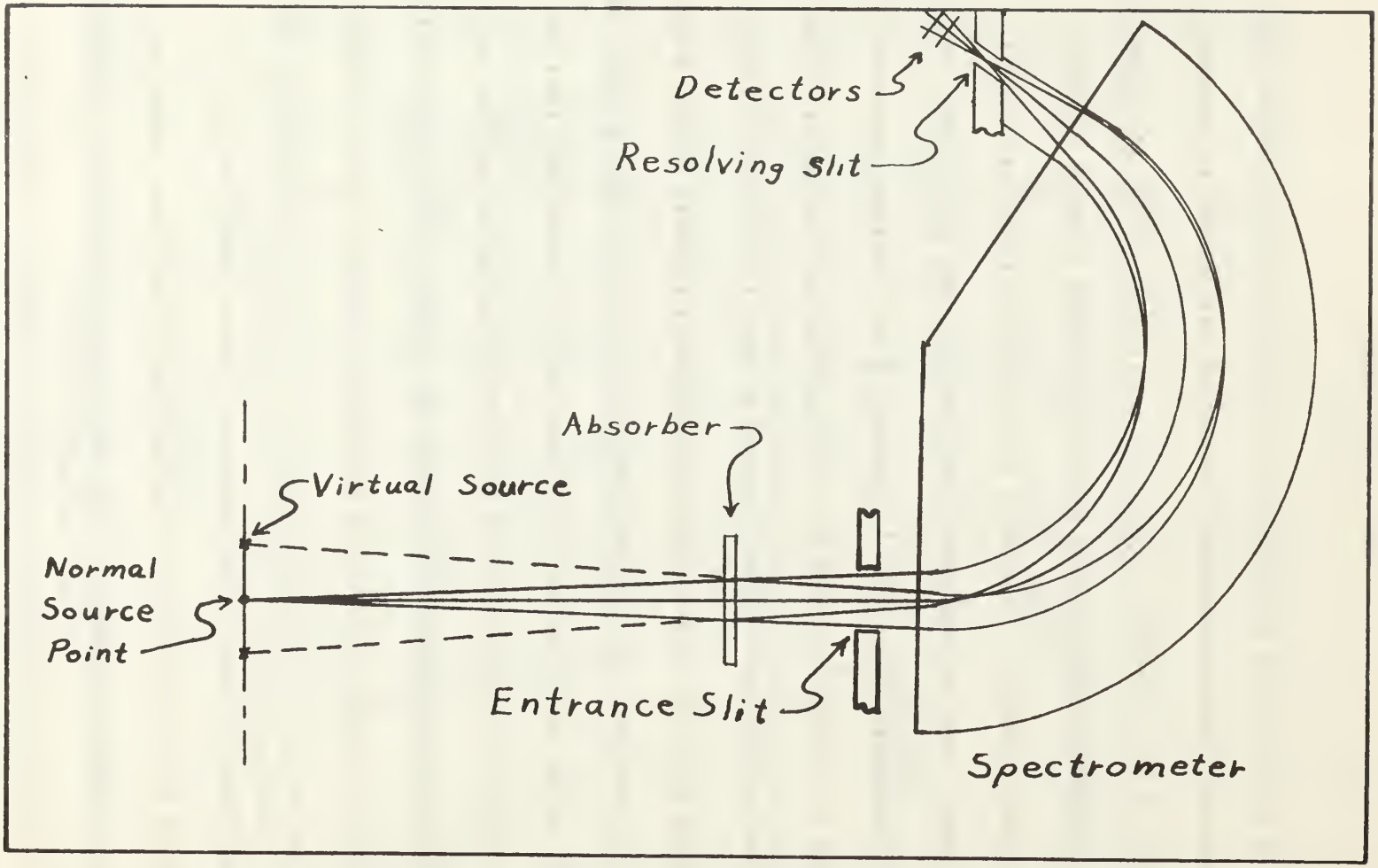

FIGURE 10 Illustration of Geometrical Resolution Effects

determination of the energy of the maximum difficult to determine since the peaks of the distribution curves are broader and statistical fluctuations on these broader peaks mask the true location. Secondly, the fact that all electrons do not travel through the absorber on paths that are perpendicular to the faces of the absorber means that there will be some path lengthening due to the geometry even if no scattering were to take place. This geometrical lengthening would be for the size of the spectrometer entrance used only about 0.2% as a maximum which corresponds to the effect on the electrons entering the spectrometer at the extreme top and bottom limits of the entrance on straight paths from the scattering foil "source". Furthermore, the probability of scattering a significant number of electrons to small angles of up to about 15 degrees increases with thickness essentially linearly so that path lengthenings of up to 3% or more could be expected to occur for a significant number of electrons if no collimation is used to exclude such electrons from entering the spectrometer. A detailed analysis of this effect is not felt justified by the quality of the present data. This effect could in part, however, explain the fact that Breuer (12) found deviations from the theory at thicknesses greater than 2 gm/cm^2.

The measurement with the absorber at the 3 cm position from the scattering foil seems to have given the best agreement both in terms of most probable loss and half width. Even so the half width of the initial energy spectrum was such that it may have also acted

to mask the effects. The initial distribution half width was for this case 325 $\pm$ 20 KeV while the theoretical half width for a monoenergetic incident beam of this energy passing through this absorber is about 577 KeV.

Factors that contributed to the width of the initial distribution to increase its energy width include (1) the upstream SEM used to monitor the electron beam current for accelerator control, (2) the 3.3 mil aluminum window at the entrance to the scattering chamber, and (3) the scattering foil used for the experiment. In addition to increasing the energy width of the initial distribution the upstream structures also cause scattering of the beam which results in a wider spatial distribution of the electrons on the scattering foil, and this results in apparent energy broadening in the data as indicated above.

With refinements in the experimental set up to move the absorbers as close as possible to the spectometer focal point without getting so close as to encounter beam edge scattering from the absorber, and perhaps collimation after the absorbers to remove electrons scattered through excessive angles where path lengthening can become significant, measurements of much better quality could be obtained. Furthermore, if the upstream obstructions could be removed for such measurements less beam spread effects should occur so that scattering at the beam edge and beam fringe induced resolution errors would be diminished.

The 16 inch spectrometer has a dispersion of 3.9 $\pm$ 0.2.

according to Oberdier (14). The exact resolution of the spectrometer cannot, however, be calculated since the exact dimensions of the beam spot are not yet known. It is estimated that the resolution of the spectrometer was of the order of 0.3% of the total energy which is acceptable for the required measurements. One problem area in this respect which could have a bearing on the most probable energy loss measurements is that there exists no system at the accelerator at this time to determine whether or not the beam intersects the scattering foil at the proper point. Errors in steering the beam into the scatterer could cause biased readings that could cause systematic errors.

The results at low energy seem to be in reasonable agreement with the results of Breuer (12) as to the most probable energy loss, and perhaps provide some insight into the factors which may have caused the discrepancies between theory and experiment as reported by Breuer. At no point in his discussion of his procedure does Breuer indicate that any form of collimation was used to limit single scattering path lengthening. This effect would obviously increase with increasing absorber thickness as was indicated in his results.

There appears to be some doubt as to the validity of assuming that the measurement of the energy difference between the initial and final experimental peaks is a valid measure of the most probable energy loss for individual electrons. The Theoretical Values in table IV are for monoenergetic electrons and therefore are the

theoretical values for the most probable loss for a single electron; however, as can be seen in figure 8, a distributed initial energy seems to cause the peak in the theoretical final distribution to fall at a lower energy than that predicted for initially monoenergetic electrons and much closer to the experimental distribution. This could also then account at least in part for the deviations from theory indicated here and by Breuer. Further experimental data of good accuracy are required for proper evaluation of this factor.

Certainly further work in this area at the USNPGS LINAC is justified, and there is good reason to believe that with the indicated refinements in the experimental arrangement that a significant addition to the literature on energy loss can be produced.

BIBLIOGRAPHY

1. Blunck, O., and K. Westphal; Zeitschrift für Physik, vol 180, page 209, (1964).

2. Landau, L.; Journal of Physics, USSR, vol. 8, page 201, (1944).

3. Blunck, O., and S. Leisegang: Zeitschrift für Physik, vol. 128, page 500, (1950).

4. Eyges, L.; Physical Review, vol 76, page 264, (1949), and vol. 77, page 81, (1950).

5. Bethe, H., and W. Heitler; Proc. Roy. Soc., Lond., Series A, vol. 146, page 83, (1934).

6. Hudson, A.; Physical Review, vol. 105, page 1, (1957).

7. Goldwasser, E. L., F. E. Mills, and A. O. Hanson; Physical Review, vol. 88, page 1137, (1952).

8. Zeigler, B.; Zeitschrift für Physik, vol. 151, page 556, (1958).

9. Sternheimer, R. M.; (a) Physical Review, vol. 88, page 851, (1952); (b) Physical Review, vol. 91, page 156, (1953); (c) Physical Review, vol. 103, page 511, (1956).

10. Yang, C. N.; Physical Review, vol. 84, page 559, (1951).

11. Rossi, B.; High Energy Particals, Prentice-Hall, New York, (1952).

12. Breuer, H.; Zeitschrift für Physik, vol. 180, page 209, (1964).

13. Kenaston, George W., C. Thomas Luke, Jr., and William C. Sones; A Multichannel Electron Detection System For Use in a Stabilized Magnetic Spectrometer, Master's Thesis, U. S. Naval Postgraduate School, (1965).

14. Oberdier, Lyn D.; The Optical Performance of the 16 Inch Magnetic Spectrometer, Master's Thesis, U. S. Naval Postgraduate School, (1967).

APPENDIX 1. Computer Program for Counting Rate Corrections

```
C      PROGRAM TO CORRECT COUNTING DATA FOR HIGH COUNTING RATE.
//FORT.SYSIN DD *
      DIMENSION E(130),EN(6,130),T(6,130),N(6,130)
      READ (5,99) M
   99 FORMAT (I3)
      READ (5,100) (E(J),EN(1,J),T(1,J),EN(2,J),T(2,J),EN(3,J),T(3,J),
     1   EN(4,J),T(4,J),EN(5,J),T(5,J),EN(6,J),T(6,J), J=1,M)
  100 FORMAT (13F5.0)
      DO 200 J=1,M
      DO 201 I=1,6
  201 N(I,J)=EN(I,J)*(1.0+EN(I,J)*3.30/(1160.0*T(I,J)+0.000001))
  200 CONTINUE
      WRITE (6,400)
  400 FORMAT (1H1, 72HENERGY                0          1          2          3
     1   4          5          /)
      WRITE (6,300) (E(J),N(1,J),N(2,J),N(3,J),N(4,J),N(5,J),N(6,J),
     1   J=1,M)
  300 FORMAT (F10.3,6I10)
      DO 90 LK=1,6
      DO 80 LS=1,M
   80 WRITE(7,900)  E(LS),N(LK,LS)
   90 CONTINUE
  900 FORMAT(' ',F7.3,6X,I5)
      STOP
      END
C-----------------------------------------------------------------------
C      DATA IN 13 FIELDS OF 5 COLUMNS EACH, FIRST FIELD IS FOR ENERGY
C      VALUE, SUBSEQUENT COLUMNS ALTERNATE COUNT, TIME, COUNT, ETC.
C      ONE DATA CARD FOR EACH ENERGY SETTING OF SPECTROMETER.
C      NEED NOT USE ALL FIELDS.
C-----------------------------------------------------------------------
```

APPENDIX 2. Computer Program for Distribution Calculations

```
C
C     PROGRAM TO CALCULATE THEORETICAL DISTRIBUTIONS FOR DISTRIBUTED
C     INITIAL ENERGY, AND PUNCH CARDS FOR PLOTTING SAME.
C
      DIMENSION FEF(400),FQO(100),EF(400)
      READ (5,20) AMP
C     READS IN AN ARBITRARY AMPLITUDE FACTOR FROM FIRST DATA CARD.
      READ (5,20) AMPX
C     READS IN THE EXPERIMENTAL AMPLITUDE FOR NORMALIZATION
   20 FORMAT (F5.0)
      READ (5,400) N
C     READS IN THE NUMBER OF DATA POINTS TO BE GIVEN FOR THE THEORETICAL
C     DISTRIBUTION DATA.
      READ (5,400) M
C     READS IN THE NUMBER OF DATA POINTS TO BE GIVEN FOR THE
C     EXPERIMENTAL INITIAL ENERGY DISTRIBUTION.
  400 FORMAT (I3)
      READ (5,399) (EIS, A, QZERO, C)
C     READS IN THE FOLLOWING:
C     EIS - THE ENERGY OF THE HIGHEST ENERGY POINT INCLUDED IN
C     THE INITIAL ENERGY DISTRIBUTION PLUS A/C.
C     B. A - THE APPROPRIATE VALUE OF THE PARAMETER AP.
C     QZERO - THE APPROPRIATE VALUE OF THE PARAMETER Q SUB ZERO
C     AS DEFINED IN THE THEORY SECTION.
C     C - A CONSTANT IN DECIMAL FORM THAT INDICATES THE NUMBER OF
C     DATA POINTS USED IN THE DISTRIBUTION IN A WIDTH OF AR UNITS OF
C     ENERGY.
  399 FORMAT (4F10.0)
      READ (5,401) (FQO(I), I=1,N)
C     READS IN THE N VALUES OF THE THEORETICAL DISTRIBUTION FOR
C     MONOENERGETIC ELECTRONS. ( ONE POINT TO A CARD).
      READ (5,401) (EF(I), I=1,M)
C     READS IN THE M VALUES FOR THE EXPERIMENTAL DISTRIBUTION OF THE
C     INITIAL ENERGY. ( ONE POINT PER CARD).
  401 FORMAT (F10.0)
      DO 499 K=1,400
  499 FEF(K)=0.000000000000000
      DO 700 J=1,N
      DO 700 I=1,M
  700 FEF(I+J-1)=FEF(I+J-1)+FQO(J)*EF(I)*AMP
      CONTINUE
      AMP=AMPX/AMAX1(FEF)*1000.
      DO 75 K=1,400
      FEF(K)=FEF(K)*0.000000000000000
   75 CONTINUE
      DO 501 J=1,N
```

```
      DO 500    I=1,M
      FEF(I+J-1)=FEF(I+J-1)+FQO(J)*FEI(I)*AMP
      B=(I+J-1)
      EF(I+J-1)=EIS-QZERO+5.0*A-B*A/C
C     NOTE THAT THE VALUE OF THE  CONSTANT WHICH IS HERE 5.0 MUST BE
C     CHANGED DEPENDING ON THE VALUE OF  THE PARAMETER B SQUARE FOR
C     THE PROGRAM TO CALCULATE PROPERLY.
      L=M+N-1
  500 CONTINUE
  501 CONTINUE
      WRITE (6,600) (EF(I), FEF(I), I=1,L)
  600 FORMAT (1H1, 18H  ENERGY      COUNT // (F10.6, F10.4))
      DO 80 LS= 1,L
   80 WRITE(7,900) EF(LS),FEF(LS)
  900 FORMAT(' ',F7.3,6X,F5.0)
      STOP
      END
```

```
C     DATA DECK IN THE FOLLOWING ORDER:
C     FIRST CARD ARBITRARY AMPLITUDE  FACTOR.
C     SECOND CARD EXPERIMENTAL FINAL DISTRIBUTION MAXIMUM AMPLITUDE.
C     FOLLOWING N CARDS THEORETICAL DISTRIBUTION FOR MONOENERGETIC.
C     FOLLOWING M CARDS INITIAL ENERGY DISTRIBUTION OF ELECTRONS.
```

```
C      PROGRAM TO CALCULATE VARIOUS DISTRIBUTION PARAMETERS AND RELATED
C      QUANTITIES.

       DIMENSION  DELEP(5,8), EIN(5),  T(8)
       DIMENSION QBAR(5,8)
       DIMENSION   B2(5,8),QZERO(5,8),A(5,8)
       DIMENSION DELEPG(5,8)
       DIMENSION ALFR(5,8)
       READ (5,104) (T(J), J=1,8)
  104  FORMAT (8F8.4)
       READ (5,102) (EIN(I),  I=1,5)
  102  FORMAT (5F10.2)
       WRITE (6, 299)
  299  FORMAT (1H1, 9HTHICKNESS,30X 20HPROBABLE ENERGY LOSS/ 1H ,
      1 7HGM/CMSQ , 45X, 3HMEV)
       WRITE (6,105) (EIN)
  105  FORMAT (1H0,11X, 5(5X,F7.2)//)
       DO 201 J=1,8
       DO 200 I=1,5
       BSQ = (EIN(I)**2+1.022*EIN(I))/((EIN(I)+0.511)**2)
       DELEP(I,J)=(0.0740*T(J)/BSQ)*(22.04+ALOG((0.0740*T(J))/BSQ)-BSQ-
      1C.0906*((3.0-ALOG10(SQRT(EIN(I)**2+1.022*EIN(I))/.511))**3.51))
       DELEPG(I,J)=DELEP(I,J)/T(J)
       QBAR(I,J) =(0.0740*T(J)/BSQ)*(21.41+ALOG(EIN(I))-BSQ-
      1C.0906*((3.0-ALOG10(SQRT(EIN(I)**2+1.022*EIN(I))/.511))**3.51))
       A(I,J)=0.154*13.0*T(J)/(24.97*BSQ)
       G=2.0*EIN(I)*(EIN(I)+0.511)*(EIN(I)+0.511)/(0.511*0.511)
       B2(I,J)=(3.00/13.0/A(I,J))*(0.0034*ALOG(  G/0.0017)+0.000065*6.0*
      1 ALOG(  G/0.000065)+0.000100*ALOG(  G/0.000020))
       QZERO(I,J)=QBAR (I,J)+A(I,J)*(1.116-ALOG(EIN(I)/A(I,J)) )
       ALFR(I,J)=T(J)*0.0014*13.0*13.0/26.97*(1.3333*ALOG(183.0/(13.0**(1
      1./3.)))+1.0/9.0)
  200  CONTINUE
  201  CONTINUE
       WRITE (6, 300) (T(J),DELEP(1,J), DELEP(2,J),  DELEP(3,J), DELEP(
      14,J), DELEP(5,J), J=1,8)
       WRITE (6,301)
       WRITE (6, 300)(T(J),DELEPG(1,J),DELEPG(2,J),DELEPG(3,J),DELEPG(4,J
      1),DELEPG(5,J),  J=1,8)
       WRITE (6,301)
       WRITE (6,300) (T(J),QBAR(1,J),QBAR(2,J),QBAR(3,J),QBAR(4,J),
      1 QBAR(5,J),  J=1,8)
       WRITE (6,301)
       WRITE (6,300) (T(J),QZERO(1,J),QZERO(2,J),QZERO(3,J),QZERO(4,J),
      1 QZERO(5,J),  J=1,8)
```

```
      WRITE (6,301)
      WRITE (6,300) (T(J),B2(1,J),B2(2,J),B2(3,J),B2(4,J),B2(5,J),J=1,
     1   8)
      WRITE (6,301)
      WRITE  (6,300) (T(J),A(1,J),A(2,J),A(3,J),A(4,J),A(5,J), J=1,8)
      WRITE (6,301)
      WRITE (6,300)  (T(J),ALFR(1,J),ALFR(2,J),ALFR(3,J),ALFR(4,J),
     1 ALFR(5,J), J=1,8)
  300 FORMAT (6(5X, F7.5))
  301 FORMAT (1H0/)
      STOP
      END
```

```
C     FIRST DATA CARD 8 THICKNESSES OF ABSORBERS  IN REQUIRED FORMAT.
C     SECOND DATA CARD 5 INITIAL ENERGY VALUES IN REQUIRED FORMAT.
```

```
C      PROGRAM TO PLOT DATA BY USE OF COMPUTER.

       REAL*8 ITITLE(12)
       DATA LB/'    '/
       DIMENSION X(100),Y(100),LABEL(2),LABEL2(2),X2(30),Y2(30)
 1000  READ(5,900) IWIDE,IHIGH,(ITITLE(I),I=1,12)
    1  READ(5,901) M,MODCUR,ITYPE,(LABEL(I),I=1,2)
       READ(5,902) (X(I),Y(I),I=1,M)
       IF(ITYPE.EQ.0) GO TO 10
       IF(M.GT.30) GO TO 20
       IF(MODCUR.GE.3) GO TO 100
   10  CALL DRAW(M,X,Y,MODCUR,ITYPE,LABEL,ITITLE,0,0,0,0,0,1,IWIDE,IHIGH,
      11,L)
       IF(L-2) 1,30,30
   20  LABEL2(2)= LABEL(2)
       LABEL2(1) = LB
       LABEL(2) = LB
       IF(MODCUR.EQ.1) GO TO 40
       IF(MODCUR.GE.3) GO TO 60
       DO 21 I=1,30
       X2(I) = X(I)
   21  Y2(I) = Y(I)
   22  CALL DRAW(30,X2,Y2,MODCUR,ITYPE,LABEL,ITITLE,0,0,0,0,0,1,0,0,0,L)
       N = 30
       IF(L-2) 23,30,30
   23  KM = M - N
   26  IF(KM.GT.30) GO TO 45
   25  DO 24 I=N,M
       X2(I-N+1) = X(I)
   24  Y2(I-N+1) = Y(I)
       CALL DRAW(KM,X2,Y2,MODCUR,ITYPE,LABEL2,ITITLE,0,0,0,0,0,1,0,0,0,L)
       IF(L-2) 1,30,30
   45  KN = N + 1
       N = N +30
       DO 46 I=KN,N
       X2(I-KN+1) = X(I)
   46  Y2(I-KN+1) = Y(I)
       LABEL(1) = LB
       LABEL(2) = LB
       GO TO 22
   40  DO 41 I=1,M
       IF(I.EQ.1) GO TO 43
       IF(X(I).GT.A) GO TO 95
       IF(X(I).LT.B) GO TO 96
```

```
      GO TO 41
   43 A = X(I)
      B=X(I)
      KL=I
      KS=I
      GO TO 41
   95 A=X(I)
      KL = I
      GO TO 41
   96 B = X(I)
      KS=I
   41 CONTINUE
      X(KS) =X(2)
      X(KL) =X(1)
      X(1) = A
      X(2) = B
      A = Y(KL)
      B = Y(KS)
      Y(KS)= Y(2)
      Y(KL) = Y(1)
      Y(1) = A
      Y(2) = B
      DO 51 I=1,30
      X2(I)  = X(I)
   51 Y2(I) = Y(I)
      N= 30
   53 CALL DRAW(30,X2,Y2,MODCUR,ITYPE,LABEL,ITITLE,0,0,0,0,0,1,IWIDE,IHI
     1GH,1,L)
      IF(L-I) 52,30,30
   52 KM = M-N
   54 IF(KN.GT.30) GO TO 75
   55 DO 56 I=N,M
      X2(I-N+1) = X(I)
   56 Y2(I-N+1) = Y(I)
      CALL DRAW(KM,X2,Y2,2,ITYPE,LABEL2,ITITLE,0,0,0,0,0,1,0,0,1,L)
      IF(L-I) 1,30,30
   75 KN = N+1
      N = N+30
      DO 76 I=KN,N
      X2(I-KN+1)=X(I)
   76 Y2(I-KN+1)=Y(I)
      LABEL(1) = LB
      LABEL(2) = LB
      MODCUR = 2
      GO TO 53
```

```
   60 DO 61 I=1,30
      X2(I) = X(I)
   61 Y2(I) = Y(I)
      N=30
   62 CALL DRAW(30,X2,Y2,2,ITYPE,LABEL,ITITLE,0,0,0,0,0,1,0,0,0,L)
      IF(L-I)63,30,30
   63 KM = M-N
   64 IF(KM.GT.30) GO TO 85
   65 DO 66 I=N,M
      X2(I-N+1) = X(I)
   66 Y2(I-N+1) = Y(I)
   67 CALL DRAW(KM,X2,Y2,3,ITYPE,LABEL2,ITITLE,0,0,0,C,C,1,0,0,0,L)
      GO TO 110
   85 KN = N+1
      N = N+30
      DO 86 I=KN,N
      X2(I-KN+1) = X(I)
   86 Y2(I-KN+1) = Y(I)
      LABEL(1) = LB
      LABEL(2) = LB
      GO TO 62
   30 WRITE(6,903)
      GO TO 110
  100 N=1
      LABEL2(1) = LABEL(1)
      LABEL2(2) = LABEL(2)
      KM=M
      GO TO 65
  110 IF(MODCUR.EQ.4) GO TO 1000
      CALL EXIT
  900 FORMAT(2I5,6A8/6A8)
  901 FORMAT(3I5,2A4)
  902 FORMAT(1X,F7.3,6X,F5.0)
  903 FORMAT('1','DRAW HAS BEEN LOCKED')
      END
```

```
------------------------------------------------------------------
C     DATA INPUTS AS INDICATED BELOW.
IWIDEIHIGH********* FIRST TITLE*****************************
************** SECOND TITLE ********************
**NP**$MOD$#TYP#LABL1LABL2
```

```
   DATA POINTS
**NP*$MOD$#TYP#LABL1LABL2
   DATA POINTS
**NP*$MOD$#TYP#LABL1LABL2
   DATA POINTS
      ALL INPUT DATA ARE RIGHT JUSTIFIED
      IWIDE :  THE WIDTH OF THE GRAPH IN INCHES 0<IWIDE<8
      IHIGH: THE HEIGHT IN INCHES 0<IHIGH<11
      NP:  NUMBER OF DATA POINTS  MAX 100
      MOD:  =1   FIRST PLOT ON GRAPH
      MOD = 2   INTERMEDIATE PLOT ON GRAPH
      MOD = 3 LAST PLOT OF LAST GRAPH
      MOD = 4 LAST PLOT OF GRAPH BUT ANOTHER GRAPH TO FOLLOW
      TYP = 0  PLOTS A CURVE
      TYP = 1 THRU 5  PLOTS POINTS WITH DIFFERENT SYMBOLS FOR EACH #
-----------------------------------------------------------------------
```

INITIAL DISTRIBUTION LIST

		No. Copies
1.	Defense Documentation Center Cameron Station Alexandria, Virginia 22314	20
2.	Library Naval Postgraduate School Monterey, California 93940	2
3.	Defense Atomic Support Agency Washington, D. C. 20305	1
4.	Professor Franz Bumiller Department of Physics Naval Postgraduate School Monterey, California 93940	12
5.	Major Royce D. Miller 4505 Grays Drive Rapid City, South Dakota 57701	1

DOCUMENT CONTROL DATA - R & D

Security classification of title, body of abstract and indexing annotation must be entered when the overall report is classified)

1 ORIGINATING ACTIVITY *(Corporate author)*

Naval Postgraduate School
Monterey, California 93940

2a. REPORT SECURITY CLASSIFICATION
UNCLASSIFIED

2b. GROUP

3 REPORT TITLE

Energy Loss of High Energy Electrons in Aluminum (U)

4 DESCRIPTIVE NOTES *(Type of report and inclusive dates)*
Thesis

5 AUTHOR(S) *(First name, middle initial, last name)*

Royce Duane Miller, Major, USA

6 REPORT DATE	7a. TOTAL NO. OF PAGES	7b. NO. OF REFS
June 1968	54	14

8a. CONTRACT OR GRANT NO.

b. PROJECT NO.

c.

d.

9a. ORIGINATOR'S REPORT NUMBER(S)

9b. OTHER REPORT NO(S) *(Any other numbers that may be assigned this report)*

10. DISTRIBUTION STATEMENT [redacted]

11. SUPPLEMENTARY NOTES

12. SPONSORING MILITARY ACTIVITY
Naval Postgraduate School
Monterey, California 93940

13. ABSTRACT

High energy electrons from the USNPGS LINAC were used to study the energy distribution characteristics of the electrons before and after passage through various thicknesses of aluminum absorbers. Data was taken for initial energies between 50 and 100 MeV, and for absorbers of thicknesses between 0.28 gm/cm^2 and 3.1 gm/cm^2. The results were compared with the theory of Blunck and Westphal, and the experimental measurements of Breuer. Geometrical factors involved in the experimental arrangement were found to have had a pronounced effect on the measurements, and refinements to the experimental conditions for future measurements of this type are indicated. Preliminary work in this direction shows that the half widths and most probable energy losses given by the theory are confirmed within experimental errors.

14 KEY WORDS	LINK A		LINK B		LINK C	
	ROLE	WT	ROLE	WT	ROLE	WT
Electrons, Energy Loss of in Aluminum						
Aluminum, Energy Loss of Electrons in